

# Chemical Knockdown of Phosphorylated p38 Mitogen-Activated Protein Kinase (MAPK) as a Novel Approach for the Treatment of Alzheimer's Disease

Seung Hwan Son,<sup>#</sup> Na-Rae Lee,<sup>#</sup> Min Sung Gee,<sup>#</sup> Chae Won Song, Soo Jin Lee, Sang-Kyung Lee, Yoonji Lee, Hee Jin Kim, Jong Kil Lee,<sup>\*</sup> Kyung-Soo Inn,<sup>\*</sup> and Nam-Jung Kim<sup>\*</sup>



Cite This: <https://doi.org/10.1021/acscentsci.2c01369>



Read Online

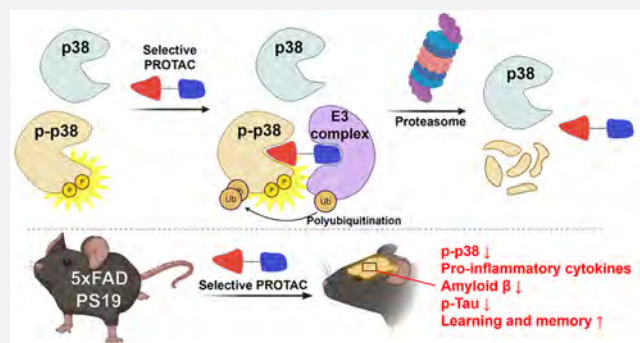
ACCESS |

Metrics & More

Article Recommendations

Supporting Information

**ABSTRACT:** Targeted protein degradation (TPD) provides unique advantages over gene knockdown in that it can induce selective degradation of disease-associated proteins attributed to pathological mutations or aberrant post-translational modifications (PTMs). Herein, we report a protein degrader, PRZ-18002, that selectively binds to an active form of p38 MAPK. PRZ-18002 induces degradation of phosphorylated p38 MAPK (p-p38) and a phosphomimetic mutant of p38 MAPK in a proteasome-dependent manner. Given that the activation of p38 MAPK plays pivotal roles in the pathophysiology of Alzheimer's disease (AD), selective degradation of p-p38 may provide an attractive therapeutic option for the treatment of AD. In the 5xFAD transgenic mice model of AD, intranasal treatment of PRZ-18002 reduces p-p38 levels and alleviates microglia activation and amyloid beta ( $A\beta$ ) deposition, leading to subsequent improvement of spatial learning and memory. Collectively, our findings suggest that PRZ-18002 ameliorates AD pathophysiology via selective degradation of p-p38, highlighting a novel therapeutic TPD modality that targets a specific PTM to induce selective degradation of neurodegenerative disease-associated protein.



## INTRODUCTION

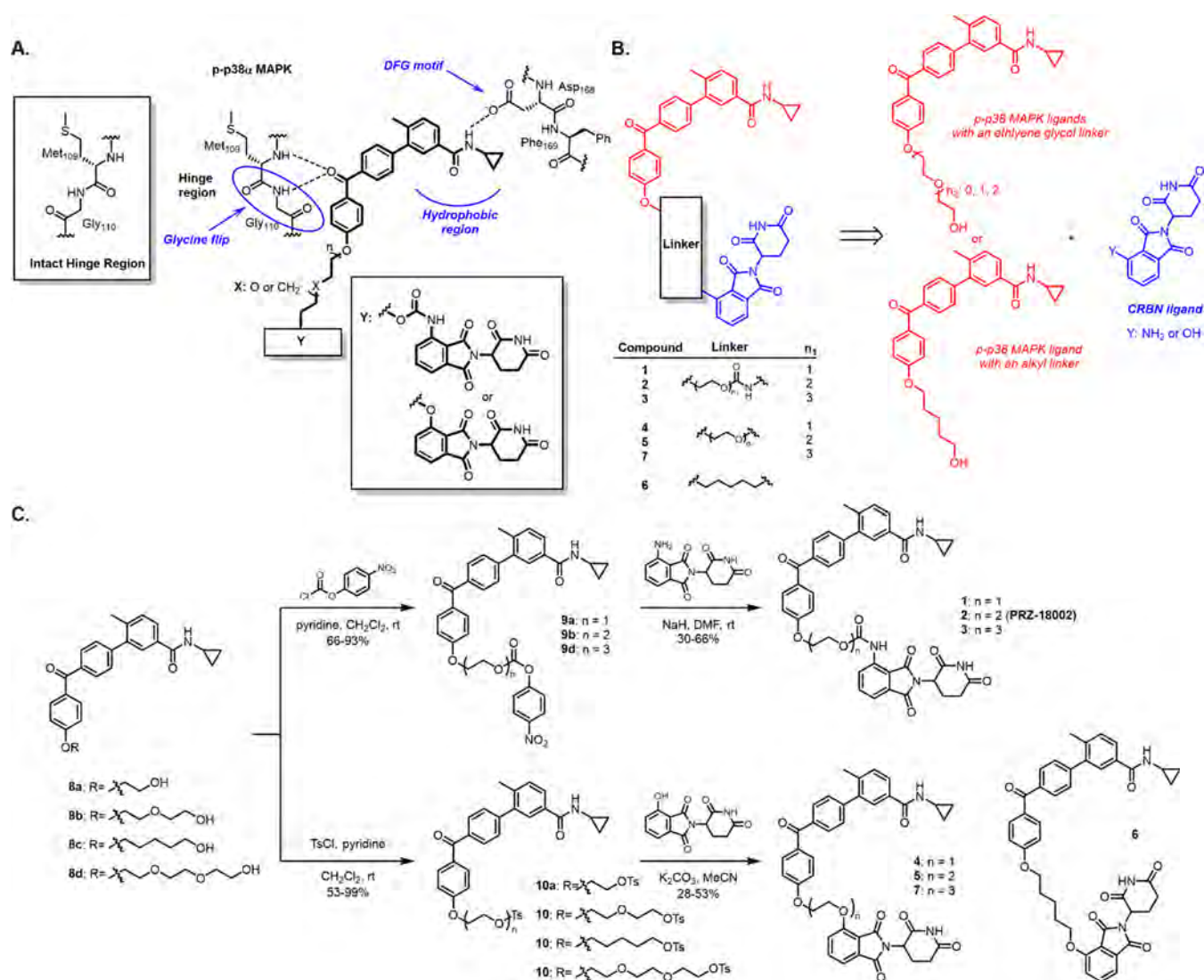
Recent progress in the field of targeted protein degradation (TPD) has proven its immense potential as a novel therapeutic modality in drug discovery. In 2015, Bradner and his colleagues devised a phthalimide-based small molecule that promotes degradation of transcriptional coactivator BRD4 by hijacking the Cereblon (CRBN) E3 ubiquitin ligase complex.<sup>1</sup> In the same year, Crews and his colleagues also reported a TPD technology recruiting the von Hippel–Lindau (VHL) E3 ligase complex, commonly referred to as proteolysis-targeting chimeras (PROTACs).<sup>2</sup> These technologies feature bifunctional small molecules that bring the proteins of interest into proximity with the E3 ubiquitin ligase complexes for ubiquitination and subsequent proteasomal degradation.<sup>3</sup> Such TPD-based small molecules have several advantages over traditional small molecule inhibitors in that they eliminate the target protein instead of modulating its function.<sup>4</sup> TPD technology thus can complement nucleic acid-based gene knockdown in removing unwanted intracellular proteins. In addition, the TPD technique can target a plethora of proteins in various compartments of the cell, including disease-causing proteins that have previously been considered undruggable with the conventional small-molecule approach. Recently, several strategies have been suggested to potentiate therapeutic efficacy of TPD technology.<sup>4</sup>

In particular, TPD molecules that recognize and bind to the protein with specific post-translational modifications (PTMs), such as phosphorylation, may be a novel strategy to induce selective degradation of pathological proteins attributed to aberrant PTMs.<sup>5</sup> However, a TPD molecule specifically targeting post-translationally modified proteins has not been reported yet.

Mitogen-activated protein kinases (MAPKs) belong to a family of serine/threonine protein kinases that participate in signaling pathways regulating cellular functions in response to various extracellular stimuli.<sup>6</sup> Among three MAPKs established in mammalian cells—extracellular signal-regulated kinase (ERK), *N*-terminal kinase (JNK), and p38—p38 has been considered to be activated mainly by pro-inflammatory cytokines and environmental stresses.<sup>7</sup> Accumulation of p-p38 through the kinase cascade is one of pathological hallmarks. It

Received: November 17, 2022

**Scheme 1. Selective p-p38 Degraders Are Designed and Synthesized on the Basis of Targeting Glycine Flip in the Hinge Region of p-p38 Active Sites: (A) Structures of Designed Degraders and Their Plausible Binding Modes. (B) Retrosynthetic Scheme of the Designed p-p38 Degraders. (C) Synthetic Scheme of Compounds 1–7**



has been reported that phosphorylated p38 (p-p38) is significantly upregulated under pathological conditions, such as chronic inflammation, thus triggering downstream signal transduction and leading to pathological deterioration.<sup>8</sup> P38 dysfunction has been implicated in a variety of medical disorders, such as neuroinflammation, ischemia, and cognitive impairment.<sup>9–12</sup> Our previous study showed that enzymatic inhibition of p38 alleviated pathological symptoms of Alzheimer's disease (AD), particularly neuroinflammation and accumulation of beta-amyloid (A $\beta$ ) and tau proteins.<sup>13</sup> The therapeutic potential of inhibiting p38 in neurodegeneration has been investigated in several clinical trials, but there has been no success yet partly due to off-target effects and insufficient efficacy.<sup>14</sup>

In this study, we use targeted protein degradation as a strategy to induce selective degradation of p-p38. Based on the phosphorylation-dependent conformational difference in p38, the glycine flip and DFG motif change, we rationally designed and synthesized a series of p-p38-degrading small molecules, consisting of a p-p38 ligand and pomalidomide that can recruit the CRBN E3 ubiquitin ligase complex. Among them, we found

that compound 2, namely PRZ-18002, displayed excellent kinase selectivity and efficiently degraded p-p38 as well as the constitutively active phosphomimetic mutant of p38 in several types of cells. The modeling study showed that PRZ-18002 nicely binds to the DFG-in conformation of p-p38 and gives adequate proximity to CRBN with the optimized linker moiety. Using a positioning device that allows us to circumvent the blood–brain barrier (BBB),<sup>15</sup> we were able to administer PRZ-18002 intranasally into the brain of 5xFAD transgenic mice that recapitulated major features of AD. Importantly, we found that PRZ-18002 induced selective *in vivo* degradation of p-p38 and ameliorated neurodegenerative symptoms including neuroinflammation, A $\beta$  deposition, and memory loss. Overall, this study highlights selective targeting of p38 bearing a specific PTM for proteasomal degradation, providing a novel therapeutic approach for the treatment of AD.

## RESULTS

**Synthesis of p-p38 Degraders.** In our previous study, we reported a series of novel p38 inhibitors that target the hinge region of p38.<sup>16</sup> The benzophenone moiety of p38 inhibitor can

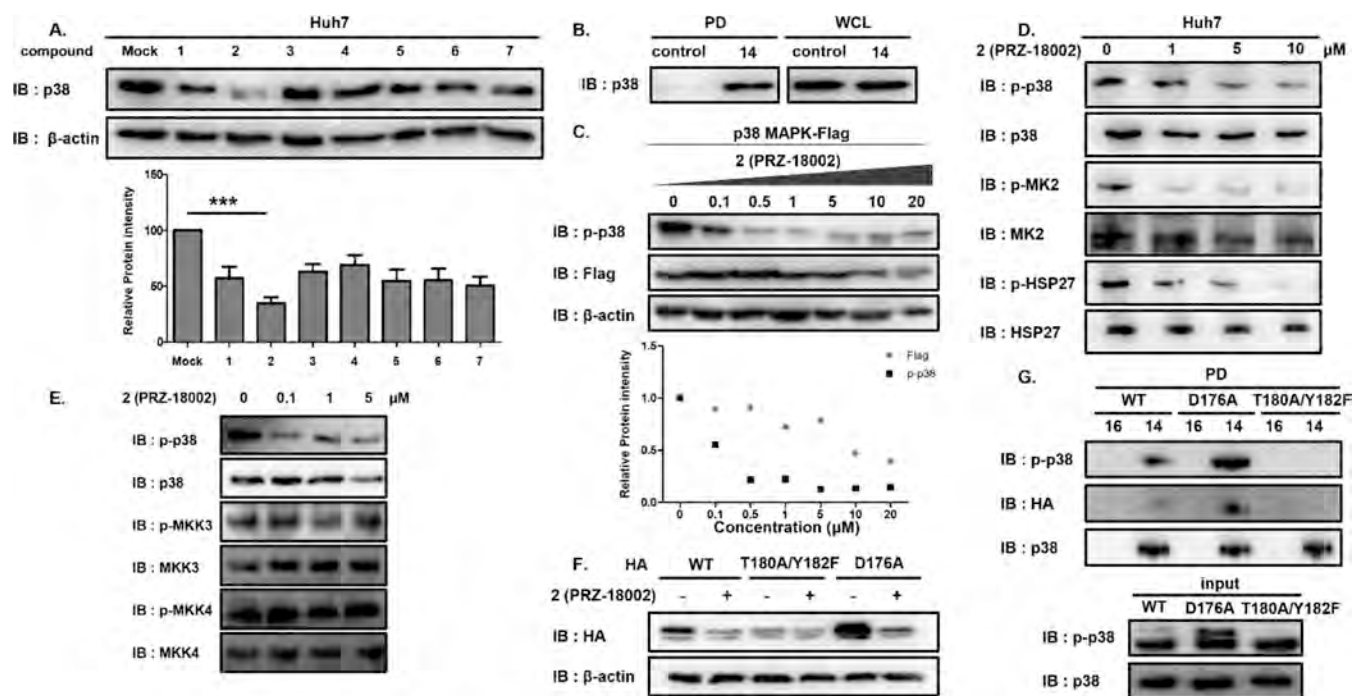


**Figure 1.** PRZ-18002 induces degradation of phospho-p38 protein in a proteasome-dependent manner. (A) Synthesized compounds were screened and PRZ-18002 successfully degrades p38. Huh7 cells were treated with p38 degraders at 10  $\mu$ M for 24 h, and cell lysates were analyzed by immunoblotting using anti-p38 antibody and anti- $\beta$  actin antibody. The bottom graph shows quantification of p38 levels. The immunoblot is representative of three independent experiments ( $n = 3$ ). Data are shown as mean  $\pm$  SEM (\*\*\*)  $P < 0.001$ .  $P$  values were calculated with analysis of variance (ANOVA). (B) p38 ligand part in 2 binds p38. Biotin-conjugate (14) of the p38 ligand part in PRZ-18002 and biotin-conjugate of benzene (16, control compound) were manufactured to confirm binding with PRZ-18002 and p38. Lysates of BV-2 cells were incubated with 20  $\mu$ M 14 or 16 at 37  $^{\circ}$ C for 2 h and then subjected to a pull-down assay. The resulting precipitates and whole cell lysates were analyzed by immunoblotting using p38 antibody. (C) PRZ-18002 preferentially degrades p-p38 over p38 in a concentration-dependent manner. HEK293T cells expressing Flag-tagged p38 were incubated with PRZ-18002 for 24 h at the indicated concentration. Cell lysates were analyzed by immunoblotting with indicated antibodies. (D) PRZ-18002 treatment results in suppression of p-pMK2 and p-HSP27 levels. Huh7 cells were treated with PRZ-18002 for 24 h at the indicated concentrations, and their lysates were analyzed by immunoblotting using p-pMK2 and p-HSP27 antibodies. (E) p-MKK3 and p-MKK3 levels are not decreased by 2, unlike p-p38. Huh7 cells were incubated with PRZ-18002 for 24 h at the indicated concentrations. Cell lysates were analyzed by immunoblotting. (F) PRZ-18002 preferentially interacts with the active form of p38. HEK293T cells expressing p38 wild-type, p38 inactive form (D180A/Y182F mutant) or p38 active form (D176A mutant) were treated with PRZ-18002 for 24 h and then were analyzed by immunoblotting. (G) p38 ligand part in PRZ-18002 selectively and preferentially binds to a phosphomimetic mutant of p38. HEK293T cells were transfected with p38 wild-type, p38 inactive form, or p38 active form followed by incubation for 24 h. Cell lysates were incubated with 14 or 16 at 4  $^{\circ}$ C for 24 h. Pull-down assays were conducted using streptavidin beads, and then the p-p38 protein level and p38 protein level were determined by immunoblotting.

form double hydrogen bonds with the NH groups of Gly110 and its adjacent linker residue Met109 at the hinge region of p38. This interaction occurs by inducing a glycine flip, in which a glycine residue undergoes rotation and replaces the position of the carbonyl oxygen with the NH group. While the amide proton of Gly110 is oriented away from the ATP-binding pocket of p38, the hydrogen bond acceptor of the inhibitor induces the glycine flip that directs the amide proton inward, leading to tight and selective binding with p38 (Scheme 1A). This flip interaction imposes high selectivity of the inhibitors to p38 because such an arrangement exists only in 9.2% of the kinome.<sup>17</sup> Interestingly, it has been reported that the intrinsic conformation of phosphorylated p38 is analogous to the structure where the flip was induced by the p38 inhibitors,<sup>18</sup> which allowed us to hypothesize that p-p38 might be a more favorable target of the inhibitors compared with their nonphosphorylated counterpart. Accordingly, in search of potent and selective degraders of phosphorylated p38, we designed and synthesized a series of chemical compounds (1–7) by conjugating the p38 inhibitor targeting a glycine flip<sup>13</sup> and pomalidomide using linkers (Scheme 1B–C and Figure S1A).

**Identification of PRZ-18002 as a Selective Degradator of p-p38.** When we tested the ability of compounds (1–7) to reduce the level of p38 protein in Huh7 cells, 2 (PRZ-18002) was shown to be the most effective degrader of p38 (Figure 1A). We also synthesized compound 14, biotin-conjugate of p38 ligand part in 2 (Figure S1B), and confirmed a robust interaction between compound 14 and p38 by a pull-down assay (Figure 1B), indicating that the p38 ligand in PRZ-18002 is responsible for the interaction with p38. In the presence of PRZ-18002, significant reduction of p-p38 was observed in a concentration-dependent manner, with a half-maximal degradation concentration ( $DC_{50}$ ) of 93 nM (Figure 1C), compared with Flag-tagged p38 ( $DC_{50}$  of 7309 nM), indicating higher selectivity of PRZ-18002 toward activated p-p38 compared with inactive p38 in the nonphosphorylated state. The docking study showed that the p38 ligand part of PRZ-18002 would nicely bind to the hinge region of the phosphorylated p38 $\alpha$  DFG-in conformation via double hydrogen bonding by glycine flip (Figure S2A, note that a more detailed interaction is shown in Figure 2E), while the compound might have a steric clash at the binding site of DFG-out (i.e., inactive) conformation (Figure S2B). PRZ-18002 also decreased the phosphorylation level of downstream targets of



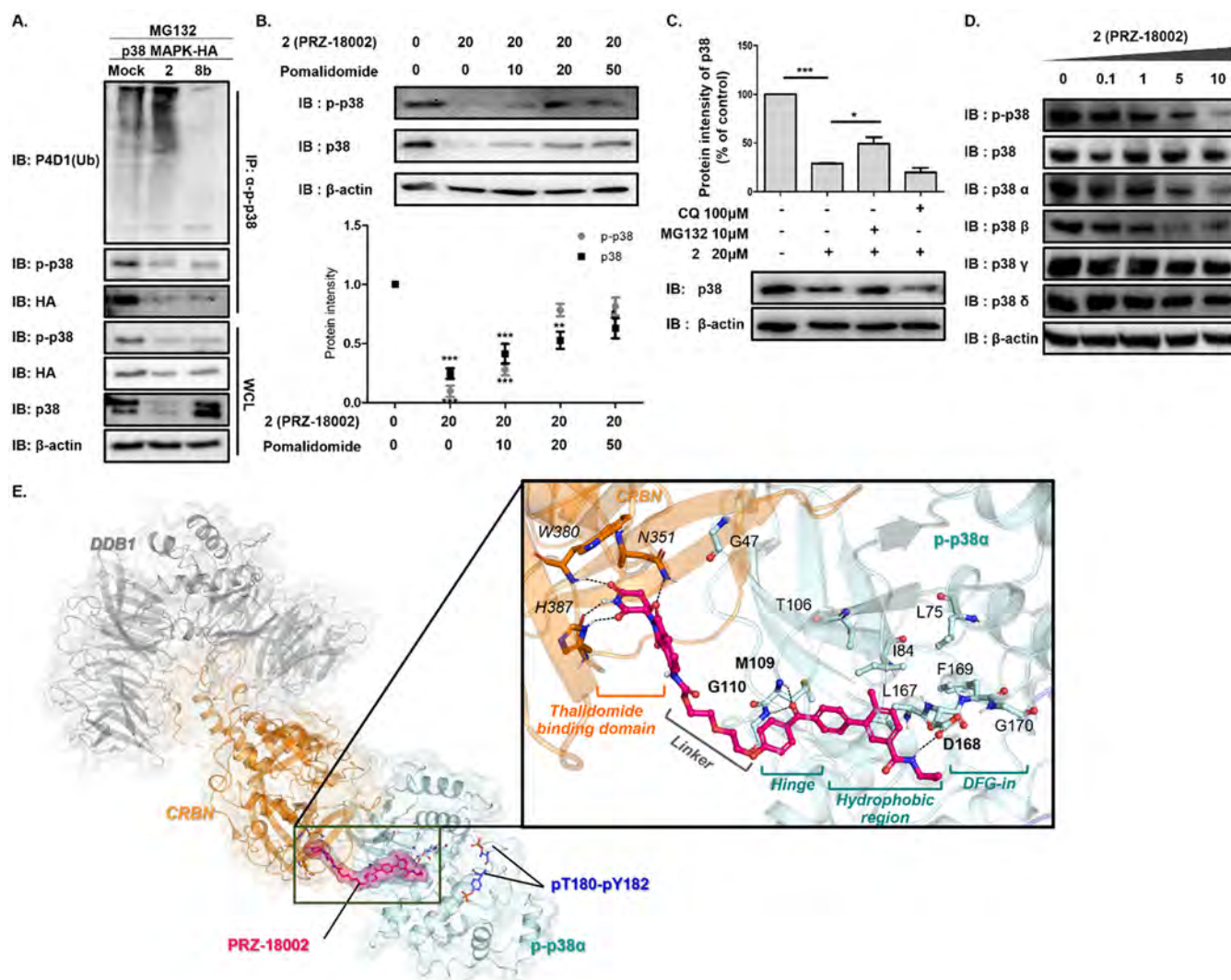


**Figure 2.** PRZ-18002 induces degradation of p-p38 and p38 protein in a proteasome-dependent manner. (A) PRZ-18002 induces ubiquitination of p-p38. HEK293T cells were transfected with p38-HA plasmid and incubated for 24 h. HEK293T cells overexpressing p38 were treated for 24 h with either compound [10  $\mu$ M PRZ-18002 or 10  $\mu$ M 8b] or DMSO together with 5  $\mu$ M MG132. An immunoprecipitation assay for each sample was performed, and the result was analyzed by immunoblotting. (B) In Huh7 cells, PRZ-18002-mediated degradation of p-p38 and p38 was significantly hindered in the presence of pomalidomide. Immunoblot analysis for p-p38 and p38 was performed after 6 h pretreatment with either DMSO or pomalidomide, followed by treatment with 2 for 24 h. Cell lysates were analyzed by immunoblotting. The immunoblot is representative of three independent experiments ( $n = 3$ ). Data are shown as mean  $\pm$  SEM ( $*P < 0.05$ ;  $**P < 0.01$ ;  $***P < 0.001$  vs control group). (C) p-p38 is degraded by PRZ-18002 in a proteasome-dependent manner. Huh7 cells were treated with DMSO or 20  $\mu$ M PRZ-18002 together with 100  $\mu$ M CQ or 10  $\mu$ M MG132. Cell lysates were analyzed with anti-p38 and anti- $\beta$  actin antibodies. The upper graph shows quantification of p38 levels. The immunoblot is representative of three independent experiments ( $n = 3$ ). Data are shown as mean  $\pm$  SEM ( $*P < 0.05$ ;  $***P < 0.001$ ). (D) p-p38 degradation by PRZ-18002 has selectivity for p38  $\alpha$  and p38  $\beta$  rather than p38  $\gamma$  and p38  $\delta$ . Huh7 cells were treated with p38 degrader at 0.1, 1, 5, 10  $\mu$ M for 24 h. Cell lysates were analyzed with antibodies as indicated. (E) Predicted binding mode of PRZ-18002 in the active p38 $\alpha$  and E3 ligase complex. The structures of the p-p38 $\alpha$ , CRBN, and DNA damage binding protein (DDB1) in E3 ligase complex are colored in cyan, orange, and gray, respectively. The phosphorylated T180 and Y182 residues in the active p38 $\alpha$  are marked as sticks with the carbon atoms in blue. The bound PRZ-18002 molecule is represented as sticks with the carbon atom in magenta. The interacting residues in p-p38 $\alpha$  and CRBN are also depicted as sticks with their residue numbers marked.

p38, MK2, and HSP27, in a concentration-dependent manner (Figure 1D). In addition, PRZ-18002 showed excellent kinase selectivity against a panel of 96 different kinases (Figure S3), which are considered to be functionally or structurally similar to p38 based on the kinome analysis and the cross reactivity analysis with other p38 inhibitors such as SB-203580, BIRB-796, and Neflamapimod (VX-745).<sup>19</sup> We also observed a substantial reduction in the protein level of p-p38 compared with other MAPKs, such as ERK, JNK, and MEK, in their phosphorylated forms (Figure S4). In addition, the phosphorylation status of

MKK3 and MKK4 kinases, upstream MAPK kinases (MAPKKs) responsible for the phosphorylation of p38, did not show any significant change upon treatment with PRZ-18002 (Figure 1E).

Collectively, these results indicated that PRZ-18002 selectively targets and reduces the level of activated p38 without affecting MAPKs or MAPKKs. We further verified the preference of PRZ-18002 on activated p38 using its constitutively active phosphomimetic mutant (D176A) and inactive mutant (T180A/Y182F).<sup>20</sup> Treatment with PRZ-18002 re-

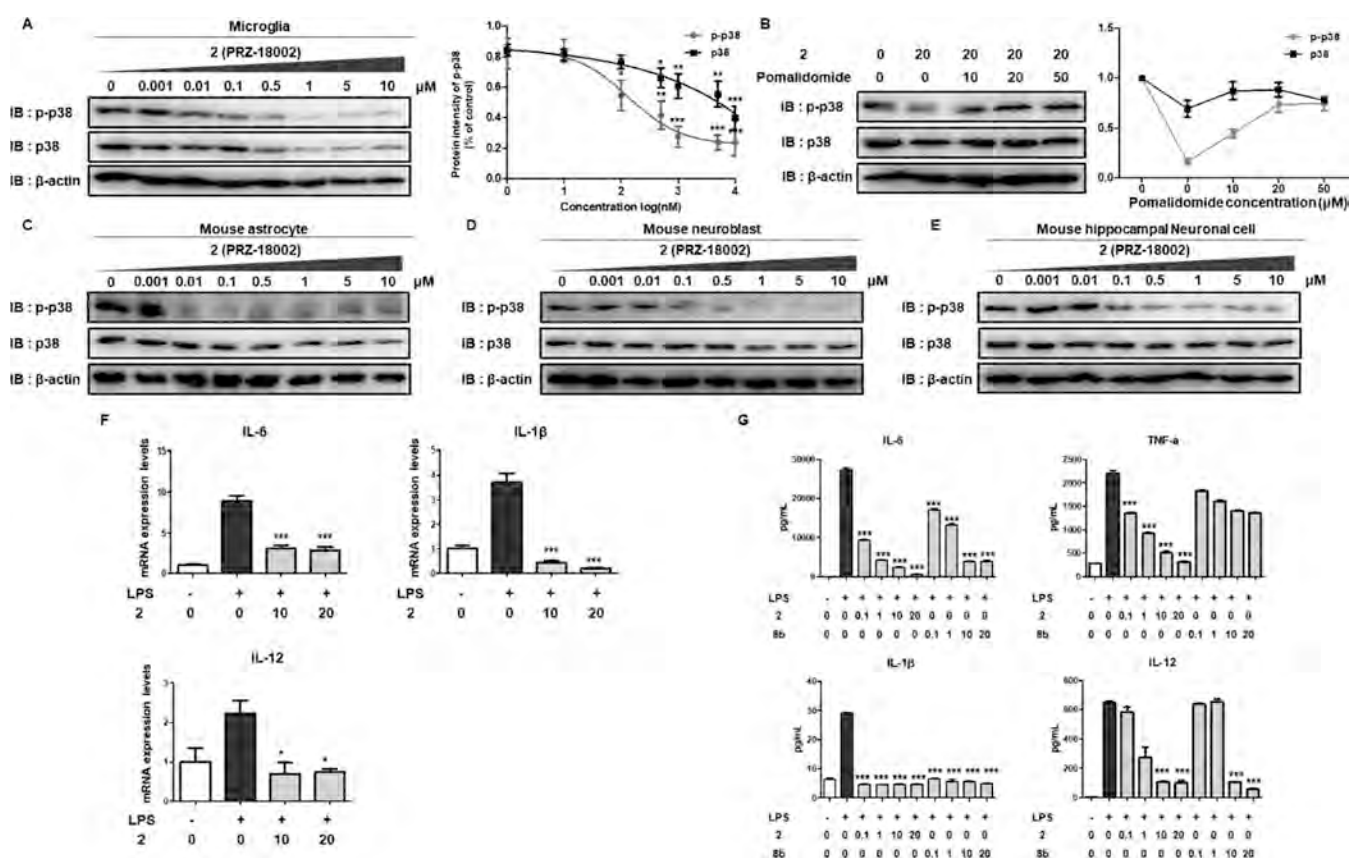


**Figure 3.** PRZ-18002 leads to decreased pro-inflammation production following degradation of both p-p38 and p38 protein in diverse brain cells. (A) PRZ-18002 induces dose-dependent decrease of p-p38 and p38. BV-2 cells, mouse microglial cells, were treated for 24 h with increasing doses of PRZ-18002, and both p-p38 and p38 levels were analyzed by immunoblotting. Right panel shows the quantification of immunoblotting. The immunoblot is representative of three independent experiments ( $n = 3$ ). Data are shown as mean  $\pm$  SEM ( $*P < 0.05$ ;  $**P < 0.01$ ;  $***P < 0.001$  vs control group). (B) In BV2 cells, PRZ-18002-mediated degradation of p-p38 and p38 was significantly hindered in the presence of pomalidomide. Cells were treated for 24 h with 20  $\mu$ M PRZ-18002 in the absence or presence of pomalidomide. (C–E) p-p38 and p38 levels upon treatment with PRZ-18002 were significantly decreased in mouse astrocyte (CD-D1a) (C), mouse neuroblast (N2a) (D), and mouse hippocampal neuronal cells (HT22) (E). (F) mRNA levels of IL-6, IL-1 $\beta$ , and IL-12 are lowered by PRZ-18002 treatment. After 16 h of PRZ-18002 treatment (0–20  $\mu$ M), BV-2 cells were stimulated with 1  $\mu$ g/mL LPS for 8 h. The mRNA level of each sample was determined by qPCR analysis. Data are shown as mean  $\pm$  SEM ( $*P < 0.05$ ;  $***P < 0.001$  vs LPS-only group). (G) Treatment with PRZ-18002 results in suppression of IL-6, IL-1 $\beta$ , IL-12, and TNF $\alpha$  levels. After 24 h of PRZ-18002 or 8b treatment (0–20  $\mu$ M), BV-2 cells were stimulated with 1  $\mu$ g/mL LPS for 24 h. The amount of each protein was measured using a cytokine Luminex assay (upper graph) and ELISA (bottom graph). The assay was performed in quadruplicate ( $n = 4$ ). Data are shown as mean  $\pm$  SEM ( $*P < 0.05$ ;  $**P < 0.01$ ;  $***P < 0.001$  vs LPS-only group).

sulted in a significant reduction of active p38 mutant (D176A) in preference to wild-type p38, whereas it showed a marginal effect on inactive p38 mutant (T180A/Y182F) (Figure 1F). In addition, a pull-down assay using compound **14**, biotin-conjugate of p38 ligand part in **2**, showed that the p-p38 ligand of PRZ-18002 selectively and preferentially binds to a phosphomimetic mutant of p38 (Figure 1G). When we proceeded to test if PRZ-18002 induces ubiquitination of p-p38 for subsequent degradation, we observed robust ubiquitination of p-p38, whereas compound **8b**, a p38 ligand lacking pomalidomide, failed to do so (Figure 2A). PRZ-18002-mediated degradation of p-p38 and p38 was significantly hindered in the presence of pomalidomide, a CRBN binder, indicating that the E3 ubiquitin ligase complex consisting of CRBN is involved in the targeted degradation of p-p38 and p38 by PRZ-18002 (Figure 2B). The effect of PRZ-18002 on degradation of p38 was diminished upon treatment with the proteasomal inhibitor MG132, while it remained unaffected by the lysosomal inhibitor chloroquine (CQ), indicating that PRZ-18002-mediated degradation of p38 occurs via a ubiquitin-proteasome system (UPS). (Figure 2C).

In addition, reduction of p38 by PRZ-18002 has selectivity for p38  $\alpha$  and  $\beta$  rather than p38  $\gamma$  and  $\delta$  (Figure 2D). In addition, compared with a p38 inhibitor, it was confirmed that the p-p38 degradation by p38 degradation ability of the p38 degrader persisted for a long time even after treatment and washing (Figure S5B). Taken together, these data demonstrate that PRZ-18002 selectively and preferentially binds to the active form of p38 and induces ubiquitination and subsequent degradation of p-p38 in a proteasome-dependent manner.

To get structural insights of the mode of action for PRZ-18002, a molecular modeling study was conducted. The p38 ligand part and the S-pomalidomide moiety of PRZ-18002 were separately docked to the X-ray crystal structures of p-p38 $\alpha$  (PDB id: 6ZQS)<sup>21</sup> and CRBN (PDB id: 5FQD),<sup>22</sup> respectively. By using the geometry of the kinase domain of casein kinase 1 bound to the E3 ligase complex (PDB id: 5FQD),<sup>22</sup> the ternary complex model of the p38 kinase domain, CRBN, DNA damage binding protein 1 (DDB1) of the E3 ligase complex were constructed. After the linker moiety was manually modeled to



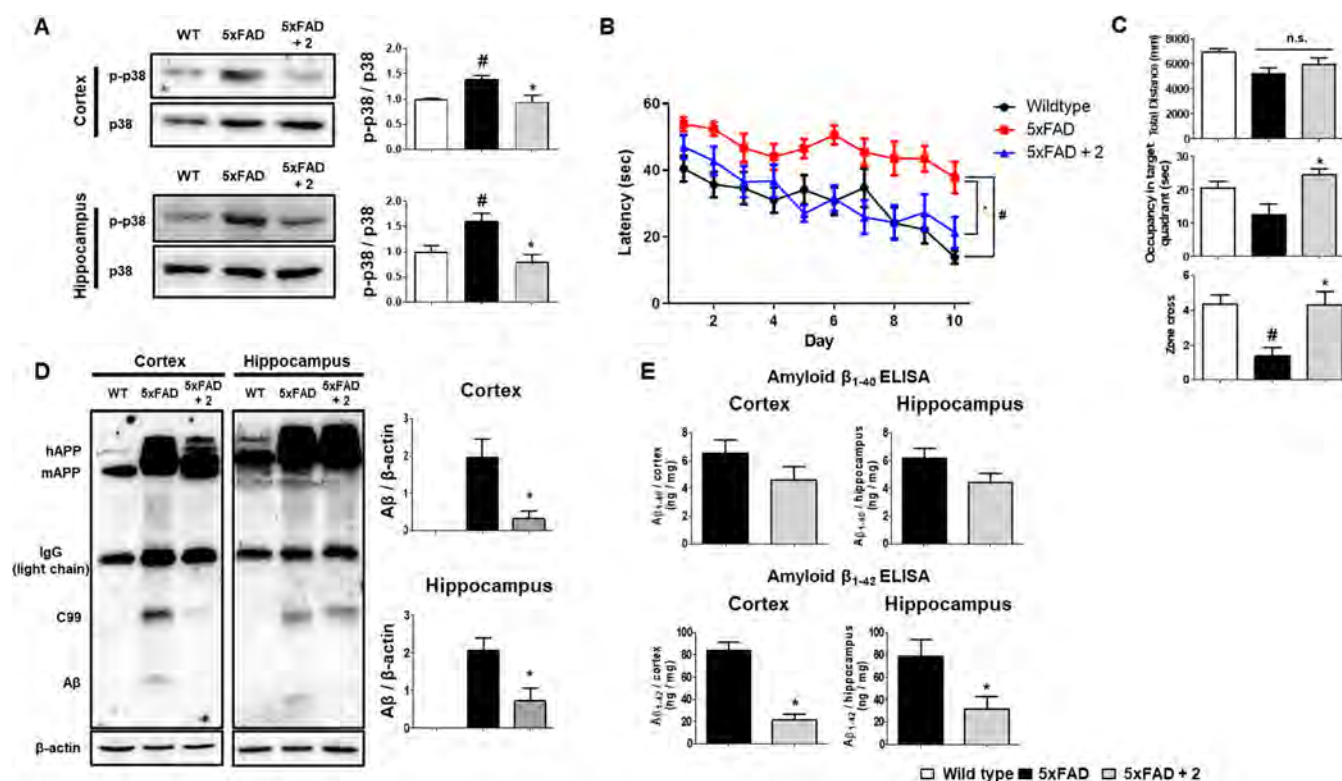


**Figure 4.** PRZ-18002 treatment diminished the phospho-p38 level and improved AD pathologies in 9-month-old 5xFAD mice. (A) Brain p-p38 levels of the mice. PRZ-18002 treated group showed significantly decreased p-p38 levels in brain, compared to the vehicle-treated 5xFAD group. Data are shown as mean  $\pm$  SEM (WT;  $n = 4$ , 5xFAD;  $n = 5$ , 5xFAD+2;  $n = 5$ , one-way ANOVA,  $^{\#}P < 0.05$  vs wild-type,  $^*P < 0.05$  vs vehicle-treated 5xFAD). (B) Morris water maze latency during the training period. The 5xFAD group took longer to arrive at the hidden platform than the wild-type group, while the PRZ-18002 treated 5xFAD group showed significantly improved performance. Data are shown as mean  $\pm$  SEM (WT;  $n = 11$ , 5xFAD;  $n = 10$ , 5xFAD+2;  $n = 10$ , GEE analysis,  $^{\#}P < 0.05$  vs wild-type,  $^*P < 0.05$  vs vehicle-treated 5xFAD). (C) Tracing analysis during probe task. Vehicle treated and PRZ-18002 treated 5xFAD group showed no significant difference in total swimming distance. Meanwhile, time spent in target quadrant and zone cross number were significantly improved than vehicle-treated 5xFAD group. Data are shown as mean  $\pm$  SEM (WT;  $n = 11$ , 5xFAD;  $n = 10$ , 5xFAD+2;  $n = 10$ , one-way ANOVA,  $^{\#}P < 0.05$  vs wild-type,  $^*P < 0.05$  vs vehicle-treated 5xFAD). (D, E) Protein levels of brain A $\beta$  were assessed by immunoblotting (D) and A $\beta$  ELISA (E) in the mice. PRZ-18002 treated 5xFAD mice showed significantly decreased A $\beta$  levels in brain, compared to vehicle-treated 5xFAD mice. Data are shown as mean  $\pm$  SEM (WT;  $n = 4$ , 5xFAD;  $n = 5$ , 5xFAD+2;  $n = 5$ , Student's  $t$  test,  $^*P < 0.05$  vs vehicle-treated 5xFAD).

connect the p38 ligand and pomalidomide part, the quaternary complex of PRZ-18002, p-p38 $\alpha$ , CRBN, and DDB1 was optimized based on energy minimization. The final structural model showed that the linker moiety of PRZ-18002 provides good proximity between the thalidomide binding domain of CRBN and the hinge region of the p38 kinase domain (Figure 2E). Especially, the benzophenone moiety interacts with M109 and G110 via double H-bonds (glycine flip), maintaining the linker's direction toward CRBN. In addition to the glycine flip, the binding mode also explains the compound's preference to the phosphorylated p38 due to the interaction with the DFG-in motif (Figure S2).

**Suppression of p38-Mediated Neuroinflammation by PRZ-18002.** In order to evaluate the potential effect of PRZ-18002 in impeding neuroinflammation, we examined if PRZ-18002 was capable of suppressing proinflammatory responses in the brain. First, in BV-2 microglial cells, we confirmed that PRZ-18002 substantially decreased p-p38 in a dose-dependent manner (Figure 3A). Consistent with previous observations in Huh7 cells (Figure 2B), PRZ-18002-mediated degradation of p-p38 in BV-2 cells was hampered in the presence of pomalidomide, suggesting that the protein degradation activity of PRZ-18002 depends on the interaction with CRBN (Figure 3B). Furthermore, PRZ-18002 was shown to have a potent

degradation activity for p-p38 over p38 in various neuronal cells, including mouse astrocytes (C8-D1A), mouse neuroblasts (N2a), and mouse hippocampal neuronal cells (HT22) (Figure 3C–E). In order to ensure PRZ-18002-induced degradation of p-p38 as a regulator of proinflammatory cytokines, we measured the mRNA expression profile of proinflammatory cytokines downstream of p38. While the mRNA levels of proinflammation cytokines such as IL-6, IL-1 $\beta$ , and IL-12 were markedly decreased (Figure 3F), the mRNA level of p38 remained unaffected upon treatment with PRZ-18002 (Figure S6A). In addition, we observed that production of proinflammatory cytokines, IL-6, IL-1 $\beta$ , IL-12, and TNF- $\alpha$ , was notably reduced in the presence of PRZ-18002 compared to compound 8b (Figure 3G). While treatment with the protein translation inhibitor cycloheximide (CHX) had no effect on the level of p-p38 and p38, cotreatment with PRZ-18002 markedly decreased the level of p-p38 (Figure S6B), suggesting that reduced level of p-p38 by PRZ-18002 does not occur from inhibiting the protein synthesis of p38.

**Alleviation of AD Pathologies by PRZ-18002 in the 5xFAD Mice.** We continued to investigate if PRZ-18002 could ameliorate AD pathologies in the mouse model, in which the 5xFAD mice aged 8 to 9 months old were treated with PRZ-18002 through intranasal injection under anesthetic conditions,

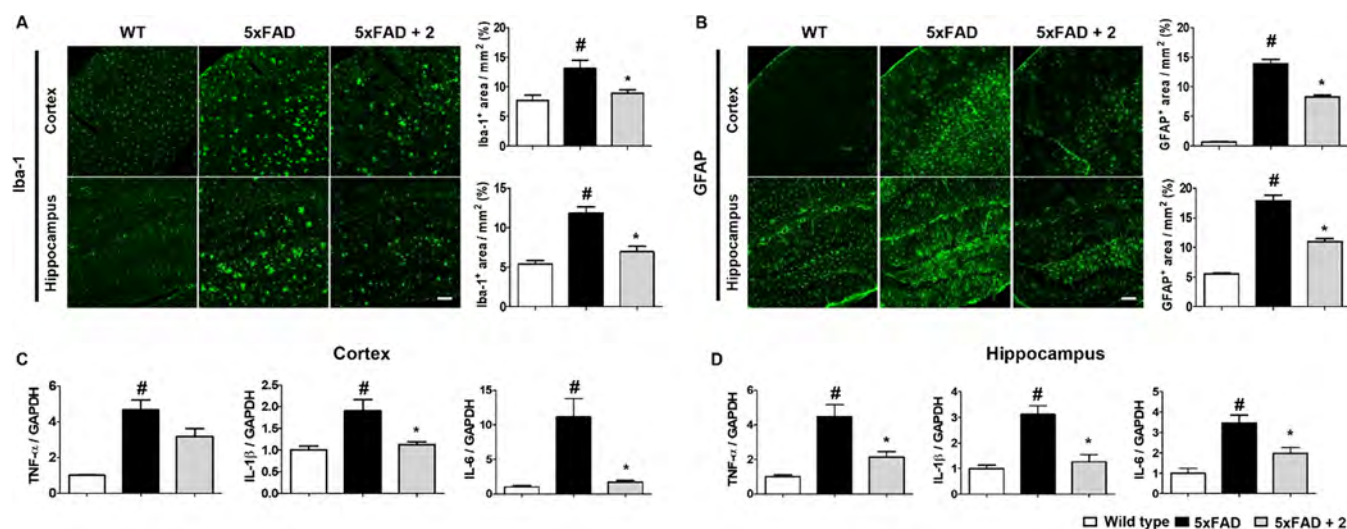


**Figure 5.** PRZ-18002 treatment diminished neuroinflammation and the production of proinflammatory cytokines. (A, B) Representative images and quantification data of Iba-1<sup>+</sup> (A) and GFAP<sup>+</sup> (B) staining in the brain. Microglia and astrocyte activations were elevated in vehicle-treated 5xFAD mice compared to wild-type mice, but these were decreased after PRZ-18002 treatment. Data are shown as mean  $\pm$  SEM (Scale bar, 100  $\mu$ m, WT;  $n$  = 4, 5xFAD;  $n$  = 5, 5xFAD+2;  $n$  = 5, one-way ANOVA, # $P$  < 0.05 vs wild-type, \* $P$  < 0.05 vs vehicle-treated 5xFAD). (C, D) mRNA levels of pro-inflammatory cytokine in mice brain. Expression of pro-inflammatory cytokines in 5xFAD group showed a significant increase compared with wild-type mice, but these were markedly decreased by PRZ-18002 treatment. Data are shown as mean  $\pm$  SEM (WT;  $n$  = 4, 5xFAD;  $n$  = 5, 5xFAD+2;  $n$  = 5, one-way ANOVA, # $P$  < 0.05 vs wild-type, \* $P$  < 0.05 vs vehicle-treated 5xFAD).

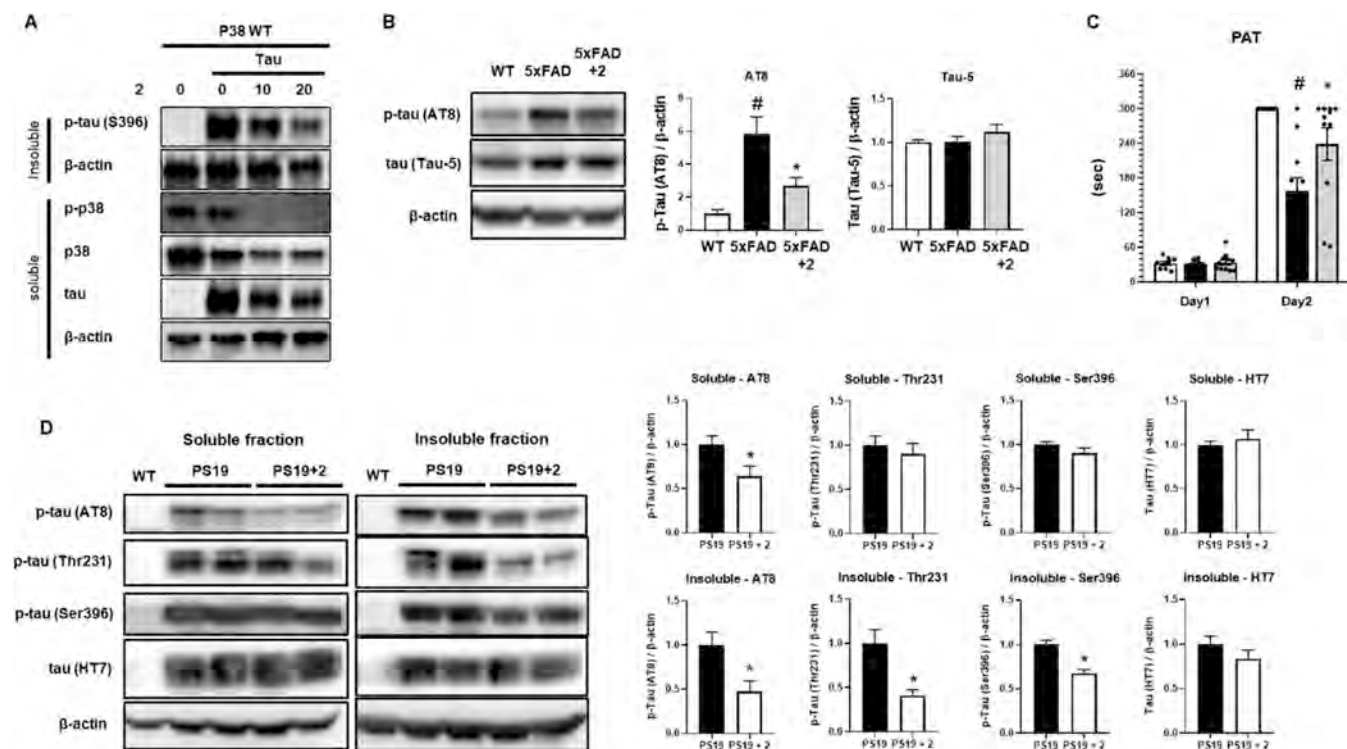


**Figure 6.** PRZ-18002 reduced aggregated p-tau protein in cells expressing tau P301L/S320F mutants and mice. (A) HEK293 cells were transfected with p38 wildtype plasmid together with or without tau P301L/S320F plasmid and incubated for 24 h. HEK293 cells overexpressing mutant tau were treated for 24 h with either compound [PRZ-18002 or 8b] or DMSO. Cell lysates were separated into an insoluble fraction and soluble fraction. Each sample of fractions was analyzed by immunoblotting using described antibodies. (B) Representative images and quantitative data of tau protein levels in the hippocampus of 5xFAD mice. Data are shown as mean  $\pm$  SEM ( $n$  = 5 per group, one-way ANOVA, # $P$  < 0.05 vs wild-type, \* $P$  < 0.05 vs vehicle-treated 5xFAD) (C) Latency time record until entering to dark compartment in PAT. Maximum time was 300-s. (WT;  $n$  = 9, PS19;  $n$  = 11, PS19+2;  $n$  = 11, one-way ANOVA, # $P$  < 0.05 vs WT, \* $P$  < 0.05 vs PS19). (D) Representative images and quantitative data of tau protein levels in the hippocampus of PS19 mice. Data are shown as the mean  $\pm$  SEM ( $n$  = 6 per group,  $t$  test, \* $P$  < 0.05 vs PS19).

which has been reported to exhibit minimal negative effects to the mice performance. We observed that PRZ-18002 was delivered to the brains of mice via intranasal injection, which

remained up to 8 h (Figure S7). Treatment with PRZ-18002 for 1 month successfully reduced the level of p-p38 in the cortex and hippocampus of the 5xFAD mice (Figure 4A). In our previous



study in the 9-months-old 5xFAD mice, we observed that a reduced level of p-p38 in the brain resulted in mitigated AD pathologies through regulation of neuroinflammatory conditions.<sup>13</sup> Similarly, PRZ-18002 treatment significantly improved the Morris Water Maze (MWM) performance of the 9-month-old 5xFAD mice (Figure 4B–C), highlighting the reconstituting effect of PRZ-18002 on spatial memory and learning in the mice model. Moreover, we confirmed that PRZ-18002 effectively diminished the level of A $\beta$  in the cortex and hippocampus of the 5xFAD mice (Figure 4D–E). Histologic analysis of A $\beta$  using thioflavin-S and anti-amyloid beta antibody also showed that deposition of A $\beta$  plaques was notably decreased in the 5xFAD mice treated with PRZ-18002 (Figure S8). Furthermore, neuroinflammation was shown to be markedly decreased in the 5xFAD mice treated with PRZ-18002 (Figure 5A–B). Consistent with previous observations in BV-2 cells (Figure 3F), we observed significant reduction in the mRNA level of proinflammatory cytokines, such as TNF- $\alpha$ , IL-1 $\beta$  and IL-6, in the cortex and hippocampus of the 5xFAD mice (Figure 5C–D). Collectively, these data suggest that PRZ-18002 alleviates neuroinflammation and pathophysiological hallmarks of AD, such as cognitive impairment and accumulation of A $\beta$ , via inducing selective degradation of p-p38 and thereby down-regulating proinflammatory signaling pathway.

**Decreased Phosphorylation of Tau by PRZ-18002 in the P301L/S320F Tau Expressing Cell and AD Mouse Model.** Together with A $\beta$ , hyper-phosphorylated tau (p-tau) is considered as one of the pathogenic proteins of AD. In order to confirm the efficacy of PRZ-18002 on tauopathy, we first conducted an experiment to determine whether the PRZ-18002 compound reduced the amount of p-tau at the cellular level. While P301L mutant tau is associated with frontotemporal dementia,<sup>23</sup> S320F mutant tau is associated with Pick's disease. It has been reported that tau phosphorylation increases when mutations occur in both sites of P301L and S320F.<sup>24</sup> We thus used the cells ectopically expressing tau with P301L and S320F mutations and confirmed that PRZ-18002 reduced the level of p-tau protein (Figure 6A).

Given that p38 MAPK inhibition may contribute to reduction of p-tau level in a cellular model, we further investigated whether PRZ-18002 ameliorated tauopathy in a mouse model of AD. First, we measured the level of p-tau in 5xFAD mice. As expected, we found that the level of p-tau (AT8, Ser396) was elevated in 5xFAD mice compared to wild-type mice. We also found that treatment of PRZ-18002 decreased the level of p-tau, while that of total tau remained unchanged (Figure 6B). Next, when we performed the passive avoidance test (PAT) and measured the level of p-tau in a tau-based AD mouse model, PS19; 7-month-old mice entered the dark compartment at day 2, unaware of the foot shock of day 1. On the other hand, PS19 mice treated with PRZ-18002 remained at the bright compartment (Figure 6C). We also observed that PRZ-18002 significantly reduced the level of p-tau (AT8, Thr231, Ser396) in the insoluble fraction of the hippocampus of PS19 mice (Figure 6D). These results collectively demonstrate that PRZ-18002 may ameliorate tauopathy as well as A $\beta$  pathology.

## DISCUSSION

TPD has been recognized as an emerging therapeutic modality for innovative drug discovery in the recent decade. The drug-like properties of chemical degraders, such as PROTACs, have paved the way to deplete pathological proteins that have previously been challenging to target with conventional small molecule

inhibitors or gene knockdown. In particular, pathologies associated with aberrant PTMs of disease-causing proteins can only be accessed by not genetic but protein knockdown. However, to date, a chemical degrader targeting PTMs of disease-relevant proteins, such as phosphorylation, has not been reported yet.

In this report, we have demonstrated that phosphorylated p38 can be targeted and sequentially eliminated by a TPD approach. For this study, we designed and synthesized small molecules preferentially targeting p-p38 over p38 by focusing on the glycine flip, a conformation that is readily formed in the hinge region of p-p38 and provides potent double hydrogen bonds with the ligands with the benzophenone moiety.<sup>18,25</sup> Through the molecular modeling, we also demonstrated that PRZ-18002 could target the DFG-in motif, a characteristic of the fully phosphorylated kinase structure, providing selectivity to active p38. We used benzophenone derivatives as a protein-binding ligand and conjugated them through biologically compatible ethylene glycol or alkyl linkers to a CRBN ligand, pomalidomide, in order to hijack the E3 ubiquitin ligase complex. We identified PRZ-18002 as the most effective degrader of p-p38, which preferentially reduced p-p38 over its nonphosphorylated counterpart. The degradation was inhibited by proteasomal inhibitor or pomalidomide, indicating that the reduced protein level of p-p38 is due to CRBN-mediated ubiquitination and proteasomal degradation. While ectopic overexpression of kinase generally triggers activation of the kinase, we observed robust reduction in the level of the ectopically expressed phosphomimetic mutant of p38, highlighting selective and effective degradation of the activated form of p38 by PRZ-18002. To the best of our knowledge, we have presented, for the first time, a chemical degrader that directly targets a specific PTM of a disease-associated protein for proteasomal degradation, further advancing a TPD approach as a novel therapeutic strategy.

Previous studies using target protein degraders for neurodegenerative disease have focused on the direct removal of aggregated pathogenic proteins such as A $\beta$  plaques, tau tangles, or mutant Huntingtins.<sup>26</sup> Recently, regulating the inflammatory conditions in the brain has been suggested as a promising therapeutic strategy for AD.<sup>27</sup> Moreover, the pivotal roles of p38 in the progression of AD have been extensively studied.<sup>28–31</sup> Previous studies have demonstrated the increased level of p-p38 in conditions associated with AD, and p38 has been reported to be related to neuroinflammatory signals for aggravation of AD. In addition, other AD-related pathophysiologicals have recently been disclosed to be associated with p38.<sup>32–35</sup> For example, formation of tau aggregates is known to be accelerated by p38-mediated phosphorylation of tau. Also, it has been reported that A $\beta$  can be scavenged via pharmacological inhibition of p38, collectively highlighting p38 as a therapeutic target of AD. A phase 2 study using a p38 inhibitor, Neflamapimod, showed that suppression of p38 can be a potential therapeutic strategy to treat AD.<sup>36</sup> Although it has failed to accomplish the primary end point in clinical trials, treatment with Neflamapimod resulted in a significant decrease of p-tau and total tau in CSF and improvement of episodic memory function, as determined by the Hopkins verbal learning test.<sup>12,37,38</sup> In particular, synaptic dysfunction was reported to be significantly improved. The p38 inhibitor has proven to be well tolerated in Phase I and II studies, conferring a novel strategy for AD treatment.<sup>39–42</sup>

Small molecules that target protein degradation against neurodegenerative disease remain an unconquered area. Small



molecule protein degraders generally consist of a target binding warhead, a linker, and a E3 ligase binding ligand, thereby giving rise to a large molecular weight unsuitable as a CNS drug.<sup>43</sup> Indeed, in our pilot trial via intraperitoneal injection, we observed neither significant improvement of memory function nor reduction of A $\beta$  deposits and p-tau in AD mice treated with PRZ-18002, partly due to its large molecular weight hampering BBB penetration. Previously, several studies have shown that intranasal delivery of chemical compounds (MW > 500) can be an efficient approach to achieving brain delivery by bypassing the BBB.<sup>44,45</sup> Furthermore, via intranasal administration combined with intravenous injection, tau-degrading peptide TH006 has shown to reduce the level of tau in the cortex of 3xTg mice.<sup>46</sup> Interestingly, it has been reported that the efficiency of brain delivery via intranasal delivery is affected by head position, and it can be robustly improved by maintaining a “mecca position”.<sup>47,48</sup> Therefore, we came up with an idea of intranasal administration of PRZ-18002 using a mouse positioning device, the Jerry seat, and successfully demonstrated that PRZ-18002 reduced the level of p-p38 in the brain of 9-month-old 5xFAD mice.<sup>15</sup> Furthermore, PRZ-18002 diminished deposition of A $\beta$ , hyper-phosphorylation of tau, reactive gliosis, and production of proinflammatory cytokines, thus resulting in improved spatial memory and learning in the AD mouse model.

Collectively, our findings suggest that TPD technology can target a specific PTM to induce selective degradation of neurodegenerative disease-associated proteins such as p-p38, demonstrating its potential as a therapeutic modality against AD.

## ■ ASSOCIATED CONTENT

### SI Supporting Information

The Supporting Information is available free of charge at <https://pubs.acs.org/doi/10.1021/acscentsci.2c01369>.

Experimental details to prepare the chemicals and methods of biological assays; supplementary tables and figures (PDF)

## ■ AUTHOR INFORMATION

### Corresponding Authors

**Jong Kil Lee** — College of Pharmacy, Kyung Hee University, Seoul 02447, Republic of Korea; Prazer Therapeutics Inc., Seoul 05836, Republic of Korea; Email: [jklee3984@khu.ac.kr](mailto:jklee3984@khu.ac.kr)

**Kyung-Soo Inn** — College of Pharmacy, Kyung Hee University, Seoul 02447, Republic of Korea; Prazer Therapeutics Inc., Seoul 05836, Republic of Korea; Email: [innks@khu.ac.kr](mailto:innks@khu.ac.kr)

**Nam-Jung Kim** — College of Pharmacy, Kyung Hee University, Seoul 02447, Republic of Korea; Prazer Therapeutics Inc., Seoul 05836, Republic of Korea; [orcid.org/0000-0003-3991-5470](https://orcid.org/0000-0003-3991-5470); Email: [kimnj@khu.ac.kr](mailto:kimnj@khu.ac.kr)

### Authors

**Seung Hwan Son** — College of Pharmacy, Kyung Hee University, Seoul 02447, Republic of Korea

**Na-Rae Lee** — Prazer Therapeutics Inc., Seoul 05836, Republic of Korea

**Min Sung Gee** — College of Pharmacy, Kyung Hee University, Seoul 02447, Republic of Korea

**Chae Won Song** — Prazer Therapeutics Inc., Seoul 05836, Republic of Korea

**Soo Jin Lee** — College of Pharmacy, Kyung Hee University, Seoul 02447, Republic of Korea

**Sang-Kyung Lee** — Department of Bioengineering and Institute of Nanoscience and Technology, Hanyang University, Seoul 04763, Republic of Korea; [orcid.org/0000-0002-1680-7218](https://orcid.org/0000-0002-1680-7218)

**Yoonji Lee** — College of Pharmacy, Chung-Ang University, Seoul 06974, Republic of Korea; [orcid.org/0000-0002-2494-5792](https://orcid.org/0000-0002-2494-5792)

**Hee Jin Kim** — Prazer Therapeutics Inc., Seoul 05836, Republic of Korea

Complete contact information is available at:

<https://pubs.acs.org/10.1021/acscentsci.2c01369>

### Author Contributions

\*S.H.S., N.-R.L., and M.S.G. contributed equally.

### Notes

The authors declare the following competing financial interest(s): Kyung Hee University and Prazer Therapeutics, Inc. have filed patent applications (PCT/KR2021/002361) based on the results of this study. The remaining authors declare no competing interests.

## ■ ACKNOWLEDGMENTS

This research was supported by the National Research Foundation (NRF) grant funded by the Korea Government (MSIT) (NRF-2022R1A2C1009252). This research was also supported by the Basic Research Laboratory Program (BRL) and Medical Research Center Program of the National Research Foundation funded by the Korean Ministry of Science, ICT and Future (NRF-2020R1A4A1016142 and NRF-2017R1A5A2014768).

## ■ REFERENCES

- (1) Winter, G. E.; Buckley, D. L.; Paulk, J.; Roberts, J. M.; Souza, A.; Dhe-Paganon, S.; Bradner, J. E. Phthalimide conjugation as a strategy for in vivo target protein degradation. *Science* **2015**, *348*, 1376–1381.
- (2) Bondeson, D. P.; Mares, A.; Smith, I. E. D.; Ko, E.; Campos, S.; Miah, A. H.; Mulholland, K. E.; Routly, N.; Buckley, D. L.; Gustafson, J. L.; et al. Catalytic in vivo protein knockdown by small-molecule PROTACs. *Nat. Chem. Biol.* **2015**, *11*, 611–617.
- (3) Stanton, B. Z.; Chory, E. J.; Crabtree, G. R. Chemically induced proximity in biology and medicine. *Science* **2018**, *359*, eaao5902.
- (4) Burslem, G. M.; Crews, C. M. Proteolysis-Targeting Chimeras as Therapeutics and Tools for Biological Discovery. *Cell* **2020**, *181*, 102–114.
- (5) Cattaneo, A.; Chirichella, M. Targeting the Post-translational Proteome with Intrabodies. *Trends in Biotechnol.* **2019**, *37*, 578–591.
- (6) Pearson, G.; Robinson, F.; Beers Gibson, T.; Xu, B.-e.; Karandikar, M.; Berman, K.; Cobb, M. H. Mitogen-Activated Protein (MAP) Kinase Pathways: Regulation and Physiological Functions. *Endocr. Rev.* **2001**, *22*, 153–183.
- (7) Johnson, G. L.; Lapadat, R. Mitogen-Activated Protein Kinase Pathways Mediated by ERK, JNK, and p38 Protein Kinases. *Science* **2002**, *298*, 1911–1912.
- (8) Herlaar, E.; Brown, Z. p38 MAPK signalling cascades in inflammatory disease. *Mol. Med. Today* **1999**, *5*, 439–447.
- (9) McLaughlin, B.; Pal, S.; Tran, M. P.; Parsons, A. A.; Barone, F. C.; Erhardt, J. A.; Aizenman, E. p38 Activation Is Required Upstream of Potassium Current Enhancement and Caspase Cleavage in Thiol Oxidant-Induced Neuronal Apoptosis. *J. Neurosci.* **2001**, *21*, 3303–3311.
- (10) Xie, Y.; Tan, Y.; Zheng, Y.; Du, X.; Liu, Q. Ebselen ameliorates  $\beta$ -amyloid pathology, tau pathology, and cognitive impairment in triple-transgenic Alzheimer's disease mice. *JBIC, J. Biol. Inorg. Chem.* **2017**, *22*, 851–865.

- (11) Zhao, Y.-w.; Pan, Y.-q.; Tang, M.-m.; Lin, W.-j. Blocking p38 Signaling Reduces the Activation of Pro-inflammatory Cytokines and the Phosphorylation of p38 in the Habenula and Reverses Depressive-Like Behaviors Induced by Neuroinflammation. *Front. Pharmacol.* **2018**, *9*, 511.
- (12) Scheltens, P.; Prins, N.; Lammertsma, A.; Yaqub, M.; Gouw, A.; Wink, A. M.; Chu, H.-M.; van Berckel, B. N. M.; Alam, J. An exploratory clinical study of p38 $\alpha$  kinase inhibition in Alzheimer's disease. *Ann. Clin. Transl. Neurol.* **2018**, *5*, 464–473.
- (13) Gee, M. S.; Son, S. H.; Jeon, S. H.; Do, J.; Kim, N.; Ju, Y.-J.; Lee, S. J.; Chung, E. K.; Inn, K.-S.; Kim, N.-J.; Lee, J. K. A selective p38 $\alpha$ / $\beta$  MAPK inhibitor alleviates neuropathology and cognitive impairment, and modulates microglia function in 5XFAD mouse. *Alzheimer's Res. Ther.* **2020**, *12*, 45.
- (14) Canovas, B.; Nebreda, A. R. Diversity and versatility of p38 kinase signalling in health and disease. *Nat. Rev. Mol. Cell Biol.* **2021**, *22*, 346–366.
- (15) Ullah, I.; Chung, K.; Beloor, J.; Lee, S.-K.; Kumar, P. A Positioning Device for the Placement of Mice During Intranasal siRNA Delivery to the Central Nervous System. *JoVE* **2019**, e59201.
- (16) Heo, J.; Shin, H.; Lee, J.; Kim, T.; Inn, K.-S.; Kim, N.-J. Synthesis and biological evaluation of N-cyclopropylbenzamide-benzophenone hybrids as novel and selective p38 mitogen activated protein kinase (MAPK) inhibitors. *Bioorg. Med. Chem. Lett.* **2015**, *25*, 3694–3698.
- (17) Martz, K. E.; Dorn, A.; Baur, B.; Schattel, V.; Goettert, M. I.; Mayer-Wrangowski, S. C.; Rauh, D.; Laufer, S. A. Targeting the Hinge Glycine Flip and the Activation Loop: Novel Approach to Potent p38 $\alpha$  Inhibitors. *J. Med. Chem.* **2012**, *55*, 7862–7874.
- (18) Yurtsever, Z.; Scheaffer, S. M.; Romero, A. G.; Holtzman, M. J.; Brett, T. J. The crystal structure of phosphorylated MAPK13 reveals common structural features and differences in p38 MAPK family activation. *Acta Crystallogr., Sect. D* **2015**, *71*, 790–799.
- (19) Hale, K. K.; Trollinger, D.; Rihanek, M.; Manthey, C. L. Differential Expression and Activation of p38 Mitogen-Activated Protein Kinase  $\alpha$ ,  $\beta$ ,  $\gamma$ , and  $\delta$  in Inflammatory Cell Lineages. *J. Immunol.* **1999**, *162*, 4246–4252.
- (20) Diskin, R.; Askari, N.; Capone, R.; Engelberg, D.; Livnah, O. Active Mutants of the Human p38 $\alpha$  Mitogen-activated Protein Kinase\*. *J. Biol. Chem.* **2004**, *279*, 47040–47049.
- (21) Kirsch, K.; Zeke, A.; Toke, O.; Sok, P.; Sethi, A.; Sebo, A.; Kumar, G. S.; Egri, P.; Poti, A. L.; Gooley, P.; Peti, W.; Bento, I.; Alexa, A.; Remenyi, A. Co-regulation of the transcription controlling ATF2 phosphoswitch by JNK and p38. *Nat. Commun.* **2020**, *11*, 5769.
- (22) Petzold, G.; Fischer, E. S.; Thomä, N. H. Structural basis of lenalidomide-induced CK1 $\alpha$  degradation by the CRL4CRBN ubiquitin ligase. *Nature* **2016**, *532*, 127–130.
- (23) Hoover, B. R.; Reed, M. N.; Su, J.; Penrod, R. D.; Kotilinek, L. A.; Grant, M. K.; Pitstick, R.; Carlson, G. A.; Lanier, L. M.; Yuan, L.-L.; et al. Tau Mislocalization to Dendritic Spines Mediates Synaptic Dysfunction Independently of Neurodegeneration. *Neuron* **2010**, *68*, 1067–1081.
- (24) Strang, K. H.; Croft, C. L.; Sorrentino, Z. A.; Chakrabarty, P.; Golde, T. E.; Giasson, B. I. Distinct differences in prion-like seeding and aggregation between Tau protein variants provide mechanistic insights into tauopathies. *J. Biol. Chem.* **2018**, *293*, 2408–2421.
- (25) Koeberle, S. C.; Romir, J.; Fischer, S.; Koeberle, A.; Schattel, V.; Albrecht, W.; Grütter, C.; Werz, O.; Rauh, D.; Stehle, T.; et al. Skepinone-L is a selective p38 mitogen-activated protein kinase inhibitor. *Nat. Chem. Biol.* **2012**, *8*, 141–143.
- (26) Wang, Y.; Jiang, X.; Feng, F.; Liu, W.; Sun, H. Degradation of proteins by PROTACs and other strategies. *Acta Pharm. Sin. B* **2020**, *10*, 207–238.
- (27) Kinney, J. W.; Bemiller, S. M.; Murtishaw, A. S.; Leisgang, A. M.; Salazar, A. M.; Lamb, B. T. Inflammation as a central mechanism in Alzheimer's disease. *Alzheimer Dement.: Transl. Res. Clin. Interv.* **2018**, *4*, S75–S90.
- (28) Hensley, K.; Floyd, R. A.; Zheng, N.-Y.; Nael, R.; Robinson, K. A.; Nguyen, X.; Pye, Q. N.; Stewart, C. A.; Geddes, J.; Markesbery, W. R.; et al. p38 Kinase Is Activated in the Alzheimer's Disease Brain. *J. Neurochem.* **1999**, *72*, 2053–2058.
- (29) Sun, A.; Liu, M.; Nguyen, X. V.; Bing, G. P38 MAP kinase is activated at early stages in Alzheimer's disease brain. *Exp. Neurol.* **2003**, *183*, 394–405.
- (30) Munoz, L.; Ammit, A. J. Targeting p38 MAPK pathway for the treatment of Alzheimer's disease. *Neuropharmacology* **2010**, *58*, S61–S68.
- (31) Lee, J. K.; Kim, N.-J. Recent Advances in the Inhibition of p38 MAPK as a Potential Strategy for the Treatment of Alzheimer's Disease. *Molecules* **2017**, *22*, 1287.
- (32) Ittner, A. A.; Gladbach, A.; Bertz, J.; Suh, L. S.; Ittner, L. M. p38 MAP kinase-mediated NMDA receptor-dependent suppression of hippocampal hypersynchronicity in a mouse model of Alzheimer's disease. *Acta Neuropathol. Commun.* **2014**, *2*, 149.
- (33) Yu, Q.; Du, F.; Douglas, J. T.; Yu, H.; Yan, S. S.; Yan, S. F. Mitochondrial Dysfunction Triggers Synaptic Deficits via Activation of p38 MAP Kinase Signaling in Differentiated Alzheimer's Disease Trans-Mitochondrial Cybrid Cells. *J. Alzheimer's Dis.* **2017**, *59*, 223–239.
- (34) Kheiri, G.; Dolatshahi, M.; Rahmani, F.; Rezaei, N. Role of p38/ MAPKs in Alzheimer's disease: implications for amyloid beta toxicity targeted therapy. *Rev. Neurosci.* **2018**, *30*, 9–30.
- (35) Muraleva, N. A.; Stefanova, N. A.; Kolosova, N. G. SkQ1 Suppresses the p38 MAPK Signaling Pathway Involved in Alzheimer's Disease-Like Pathology in OXYS Rats. *Antioxidants* **2020**, *9*, 676.
- (36) Prins, N. D.; Harrison, J. E.; Chu, H.-M.; Blackburn, K.; Alam, J. J.; Scheltens, P.; et al. A phase 2 double-blind placebo-controlled 24-week treatment clinical study of the p38  $\alpha$  kinase inhibitor neflamapimod in mild Alzheimer's disease. *Alzheimer's Res. Ther.* **2021**, *13*, 106.
- (37) Alam, J.; Blackburn, K.; Patrick, D. Neflamapimod: Clinical Phase 2b-Ready Oral Small Molecule Inhibitor of p38 $\alpha$  to Reverse Synaptic Dysfunction in Early Alzheimer's Disease. *J. Prev. Alzheimers Dis.* **2017**, *4*, 273–278.
- (38) Germann, U. A.; Alam, J. J. P38 $\alpha$  MAPK Signaling—A Robust Therapeutic Target for Rab5-Mediated Neurodegenerative Disease. *Int. J. Mol. Sci.* **2020**, *21*, 5485.
- (39) Dong, Y.; Li, X.; Cheng, J.; Hou, L. Drug Development for Alzheimer's Disease: Microglia Induced Neuroinflammation as a Target? *Int. J. Mol. Sci.* **2019**, *20*, 558.
- (40) Fu, W.-Y.; Wang, X.; Ip, N. Y. Targeting Neuroinflammation as a Therapeutic Strategy for Alzheimer's Disease: Mechanisms, Drug Candidates, and New Opportunities. *ACS Chem. Neurosci.* **2019**, *10*, 872–879.
- (41) Lee, G.; Cummings, J.; Decourt, B.; Leverenz, J. B.; Sabbagh, M. N. Clinical drug development for dementia with Lewy bodies: past and present. *Exp. Opin. Invest. Drugs* **2019**, *28*, 951–965.
- (42) Cummings, J.; Lee, G.; Ritter, A.; Sabbagh, M.; Zhong, K. Alzheimer's disease drug development pipeline: 2020. *Alzheimer's Dement.: Transl. Res. Clin. Interv.* **2020**, *6*, e12050.
- (43) Ding, Y.; Fei, Y.; Lu, B. Emerging New Concepts of Degradation Technologies. *Trends Pharmacol. Sci.* **2020**, *41*, 464–474.
- (44) Dhuria, S. V.; Hanson, L. R.; Frey, W. H., 2nd. Intranasal delivery to the central nervous system: mechanisms and experimental considerations. *J. Pharm. Sci.* **2010**, *99*, 1654–1673.
- (45) Ullah, I.; Chung, K.; Oh, J.; Beloor, J.; Bae, S.; Lee, S. C.; Lee, M.; Kumar, P.; Lee, S. K. Intranasal delivery of a Fas-blocking peptide attenuates Fas-mediated apoptosis in brain ischemia. *Sci. Rep.* **2018**, *8*, 15041.
- (46) Chu, T. T.; Gao, N.; Li, Q. Q.; Chen, P. G.; Yang, X. F.; Chen, Y. X.; Zhao, Y. F.; Li, Y. M. Specific Knockdown of Endogenous Tau Protein by Peptide-Directed Ubiquitin-Proteasome Degradation. *Cell Chem. Biol.* **2016**, *23*, 453–461.
- (47) Merkus, P.; Ebbens, F. A.; Muller, B.; Fokkens, W. J. Influence of anatomy and head position on intranasal drug deposition. *Eur. Arch. Oto-Rhino-Laryngol.* **2006**, *263*, 827–832.
- (48) Wu, H.; Hu, K.; Jiang, X. From nose to brain: understanding transport capacity and transport rate of drugs. *Exp. Opin. Drug Delivery* **2008**, *5*, 1159–1168.